Design and Control of an Active Reset Circuit for Pulse Transformers

D. Bortis, J. Biela and J. W. Kolar
Power Electronic Systems Laboratory, ETH Zurich
Physikstrasse 3, 8092 Zurich, Switzerland

ABSTRACT

In pulse modulators applying pulse transformers reset circuits are used to achieve optimal utilization of the core material, which results in lower costs, downsized pulse transformer/system volume and therefore in an improved pulse behavior due to the smaller parasitics. Because of its simplicity the most common method to reset the core is a dc reset circuit, where a dc current is used to premagnetize the core. However, the dc reset circuit - even with an optimal design - leads to significant losses in the freewheeling path. By applying an active reset method the losses due to the passive reset circuit can be reduced significantly. So far, only the theoretical behavior of the active reset circuit has been examined. Therefore, the detailed design and measurement results are presented in this paper. Furthermore, a new control method for achieving symmetrical flux swings in the core is presented.

Index Terms — **Pulse Transformer, Reset Circuit, Solid State Modulator, Energy Recovery, Premagnetization, Symmetrical Flux Swing.**

1 INTRODUCTION

IN pulsed power systems utilizing pulse transformers for voltage conversion, as shown in Figure 1, the repetitive unipolar voltage pulses lead to an unipolar flux swing in the core material. In these cases the core material of the pulse transformer is not optimally utilized and according to (1) the core volume is approximately twice as big as with a bipolar excitation for the same pulse parameters.

$$V_{DC}=N_1\frac{d\Phi}{dt}=N_1A_{Fe}\frac{dB}{dt}\Rightarrow A_{Fe}=\frac{V_{DC}}{N\frac{dB}{dt}} \qquad (1)$$

A bipolar operation of the transformer could be achieved with a reset circuit - dc reset or active reset - which premagnetizes the core to a negative flux density before the pulse is generated. The dc reset circuit, which is widely used because of its simplicity [1, 2], leads to significant losses in the freewheeling path even if the design of the dc reset circuit is optimized for minimal losses [3]. In order to reduce the losses and consequently the stress in the freewheeling diode an active reset circuit has been proposed [4-7]. In the active reset circuit the stored energy in the magnetizing inductance and in the leakage inductance can almost completely be recovered and reused for premagnetizing the transformer for the next pulse. This leads to a significant reduction of the losses due to the premagnetization and an improved efficiency of the pulse modulator. There, it is important to note that in active reset circuits a small inverted output voltage (10%-20% of the pulse voltage depending on the design) occurs at the output during pre-/demagnetization. Therefore, loads with a diode characteristic, as for example klystrons or loads with a series diode, are required to achieve an efficient active premagnetization.

In **Section 2** the operation of the active reset circuit is explained in detail and advantages of the active reset method compared to the dc reset circuit are highlighted. Thereafter, in **Section 3** the design equations for the system are derived and it is shown that the active reset circuit automatically balances the flux swing in the core in cases, where the losses in the system are low.

If the losses are higher, then the active reset circuit is still self-stabilizing, but the flux swing tends to be more and more asymmetric. In order to achieve a symmetric flux swing the premagnetization current of the core has to be actively controlled. Therefore, in **Section 4** a new control method for active reset circuits is explained. Thereafter, the design and experimental results of the active reset circuit for the 20MW, 5µs power modulator with the specifications given in Table 1 are presented in **Section 5**.

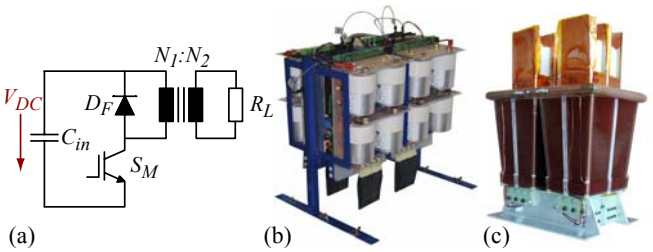

Figure 1 **(a)** Schematic of the realized solid state power modulator utilizing a pulse transformer, **(b)** Pulse generator unit with four parallel connected IGBT modules and **(c)** step up pulse transformer.

Manuscript received on X Month 2005, in final form XX Month 2005.

Table 1 Specification of the realized 20MW solid state power modulator with active reset circuit.

DC link Voltage V_{DC}	1000V
Output Voltage V_{out}	200kV
Pulse Duration T_{pulse}	5µs
Output Power P_{out}	20MW
Repetition Frequency f_{rep}	200Hz
Magnetizing Inductance L_{mag}	2.5µH
Magnetizing Current I_{Mag}	±1kA
Turns ratio N_1:N_2	1:200

2 ACTIVE RESET CIRCUIT

In Figure 2 the schematic of the power modulator with the active reset circuit is shown for a load with diode characteristic, as for example a klystron, which is not negatively influenced by the inverted output voltage during the pre-/demagnetization [4, 8]. Due to the diode characteristic no current will flow through the load during pre-/demagnetization.

The active reset circuit consists of a freewheeling diode D_F, a series capacitor C_R for storing the recovered energy and a switch S_R for premagnetizing the transformer core. The damping resistor R_D usually could be omitted, since the resistance of the interconnections already damps oscillations.

First, to premagnetize the transformer core the capacitor C_R has to be charged (e.g. by a boost converter, as will be shown later) to a specific voltage level V_{CR}. In the considered case the capacitor voltage VCR can be varied between 100V and 200V (= 10% - 20% of V_{DC}). Then, during the premagnetization interval T_{Premag} the switch S_R is closed and the premagnetization current I_{Mag} starts to flow in the primary winding of the transformer (cf. Figure 3 a) & Figure 4). There, the current I_{Mag} is flowing in opposite direction as the load current and generates a magnetic flux, which is in the opposite direction than the flux induced by the voltage pulse.

Consequently, the energy stored in the capacitor C_R is transferred to the magnetizing inductance L_{Mag}, which results in a linear current slope of I_{Mag}, if an approximately constant capacitor voltage V_{CR} is assumed. In this case, the current level $I_{mag,1}$ reached at t_1 (cf. Figure 4) can be calculated by (2).

$$I_{Mag,1} = \frac{V_{CR} \cdot T_{Premag}}{L_{Mag}} \qquad (2)$$

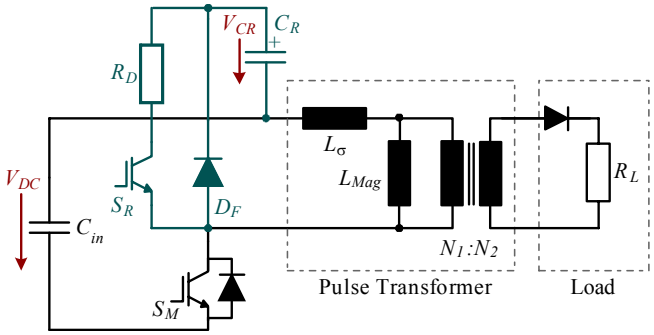

Figure 2 Schematic of the power modulator with the active reset circuit.

In order to achieve a required nominal magnetizing current $I_{Mag,nom}$, with (2) it is also possible to calculated the length of the premagnetization interval T_{Premag} if V_{CR} is known.

As soon as $I_{Mag,1} = I_{Mag,nom}$ is reached, switch S_R is turned off at t_1. Thereafter, a short interlocking delay T_I follows before S_M is turned on in order to avoid a short circuit. During T_I the magnetizing current I_{Mag} flows either via the DC link capacitor and the antiparallel diode of the main switch S_M or through the load in positive direction. Through which path the current flows depends on the ratio of the voltage drop across the klystron, which would be caused by the magnetizing current, to the DC link voltage (cf. Figure 3 b)). The klystron voltage can be calculated with (3), where k_p is the perveance of the klystron [9, 10].

$$I_k = k_p \cdot V_k^{\frac{3}{2}} \quad \Rightarrow \quad V_k = \left(\frac{I_k}{k_p}\right)^{\frac{2}{3}} \qquad (3)$$

Due to the transformation ratio of the transformer, the premagnetization current I_{Mag} is usually more than a factor of ten smaller than the load current transformed to the primary. Therefore, also the klystron voltage V_k during the premagnetization time T_{Premag} transformed to the primary is much smaller than the DC link voltage V_{DC}. For a magnetizing current I_{Mag} of 1000A on the primary the klystron voltage V_k' reflected to the primary would only be approximately 60V in the considered case. Consequently, the premagnetization current I_{Mag} will freewheel through the klystron and not via the DC link capacitor during the interlocking delay T_I.

Due to the relative small klystron voltage V_k' reflected to the primary (V_k' << V_{DC}, cf. Figure 2), which is proportional to the voltage across the magnetizing inductance, the rate of change of the magnetizing current during the interlocking delay T_I is small. Therefore, the length of the interlocking delay T_I is not very critical for the operation of the active reset circuit. As a result of the small load current I_k during T_I also the losses in the klystron during the freewheeling period will be small, which - in the considered system - are 36W for a pulse repetition rate of f_{rep} = 200Hz and a interlocking delay of T_I = 3µs.

On the other hand, the energy stored in the leakage inductance causes a current, which flows via the DC link capacitor C_{in} and the antiparallel diode of the main switch S_M.

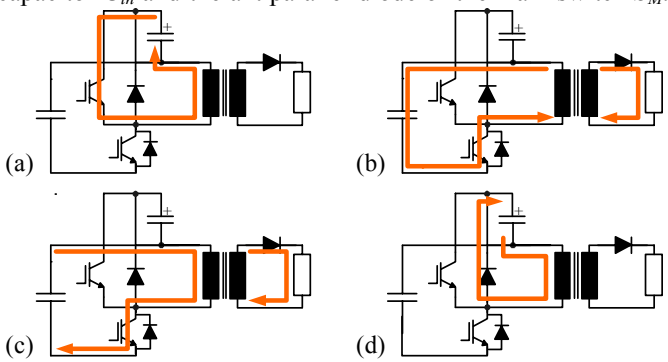

Figure 3 Current paths during **(a)** the premagnetization time T_{Premag}, **(b)** the interlocking delay T_I, **(c)** the pulse duration T_{Pulse} and **(d)** the demagnetization time T_{Demag}.

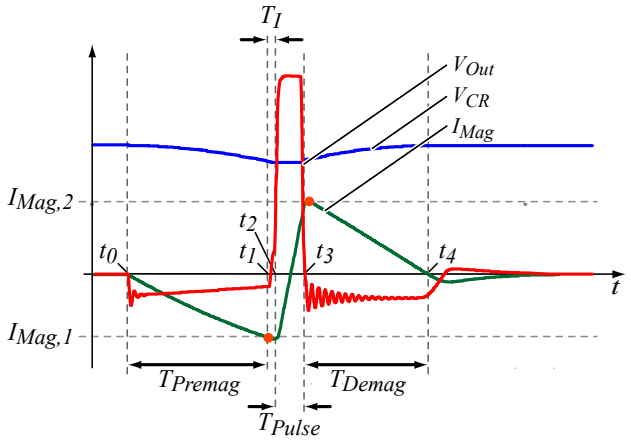

Figure 4 Current and voltage waveforms for the active premagnetization for one pulse period.

Due to the small leakage inductance and the relatively large DC link voltage V_{DC} compared to the klystron voltage V_k', the leakage current through the input stage decreases rapidly. In the case, where the main switch is turned on while the current through the input stage is still flowing via the antiparallel diode of S_M, the turn on losses of S_M could be reduced significantly (ZVS).

After the interlocking delay T_I the pulse is generated by turning on the main switch S_M at time instant t_2. During the pulse the magnetizing current is linearly ramping up from $I_{Mag,1}$ to $I_{Mag,2}$ as shown in Figure 3 c) and Figure 4 due to the constant pulse voltage V_{DC}.

After the pulse, during T_{Demag}, the energy stored in the magnetizing inductance L_{Mag} (and the part of the energy stored in the leakage inductance L_σ, which is not dissipated in S_M during turn off) is fed back to the reset capacitor C_R via the freewheeling diode D_F (cf. Figure 3 d) and Figure 4), as the magnetizing current could not flow via the load due to the diode characteristic.

Since the reset capacitor voltage V_{CR} is much larger than the forward voltage of the diode D_F, the losses in the diode can be kept small and the duration for demagnetization T_{Demag}, which is mainly defined by the capacitor voltage V_{CR}, is short. For an almost constant capacitor voltage V_{CR} the freewheeling interval can be approximated by (4).

$$T_{Demag} = L_{Mag} \cdot \frac{I_{Mag,2}}{V_{CR}} \tag{4}$$

3 SELF-STABILIZATION OF THE FLUX SWING

If the core is excited symmetrically from $-I_{Mag}$ to I_{Mag}, for an ideal system without losses, the energy recovered after the pulse will be the same as the energy, which was required to premagnetize the core (cf. Figure 5 a)).

$$\frac{1}{2} L_{mag} I_{mag,1}^2 = \frac{1}{2} L_{mag} I_{mag,2}^2 \tag{5}$$

Therefore, after the freewheeling interval T_{Demag} the reset capacitor C_R is recharged to the same voltage level as before the pulse was generated. In practice, however, the voltage across C_R after the pulse will be below the voltage level as before the pulse due to the losses in the freewheeling diode D_F, the switch S_R, the bus bar, the winding and the core. The voltage drop (7), caused by the system losses E_{Losses}, can be calculated by means of the difference of the stored energy in the capacitor C_R at t_2 and t_3 with (6), which can be solved with $V_{CR,t3} = V_{CR,t2} - \Delta V_{CR}$.

$$E_{Losses} = \frac{1}{2} C_R V_{CR,t2}^2 - \frac{1}{2} C_R V_{CR,t3}^2 \tag{6}$$

$$\Delta V_{CR} = V_{CR,t2} - \sqrt{V_{CR,t2}^2 - \frac{2E_{Losses}}{C_R}} \tag{7}$$

In cases, where the magnetizing current I_{Mag} directly before the pulse and after the pulse are not equal, energy is stored/removed in/from the magnetizing inductance L_{Mag} during the pulse interval as shown in Figure 5. The amount of energy ΔE_{Pulse} depends on the current level $I_{Mag,1}$ in relation to $I_{Mag,2}$.

For example, the energy variation ΔE_{Pulse} for a symmetric flux swing in the magnetizing inductance would be zero if $|I_{Mag,1}| = |I_{Mag,2}|$ and consequently $1/2 \cdot L_{mag} \cdot I^2_{mag,1} = 1/2 \cdot L_{mag} \cdot I^2_{mag,2}$. In (8) the relation between $I_{Mag,1}$ and the additional pulse energy ΔE_{Pulse} stored in the magnetizing inductance L_{Mag} is given.

$$\begin{aligned} \Delta E_{Pulse} &= \frac{1}{2} L_{Mag} I_{Mag,2}^2 - \frac{1}{2} L_{Mag} I_{Mag,1}^2 \\ &= \frac{1}{2} L_{Mag} \left(\Delta I_{Mag}^2 - 2 \Delta I_{Mag} I_{Mag,1} \right) \end{aligned} \tag{8}$$

If the premagnetization interval T_{Premag} is set to a fix value determined with (2), a variation in capacitor voltage V_{CR} will lead to a variation in the magnetizing current $I_{Mag,1}$. Whenever the capacitor voltage V_{CR} is below the nominal voltage $V_{CR,nom}$ then the magnetizing current $I_{Mag,1}$ is smaller than the nominal magnetization current $I_{Mag,nom}$. Consequently, this results in an asymmetric flux swing, where ΔE_{Pulse} is bigger than zero (cf. (8) respectively Figure 5 b)). Therefore, the additional energy ΔE_{Pulse} stored in the magnetizing inductance L_{Mag} will be fed back to the reset capacitor V_{CR} and depending on the system losses E_{Losses} the capacitor voltage V_{CR} will increase if $\Delta E_{Pulse} > E_{Losses}$ or will drop if $\Delta E_{Pulse} < E_{Losses}$.

Assuming for example $\Delta E_{Pulse} < E_{Losses}$, the voltage V_{CR} will decrease and for the next pulse the current $I_{Mag,1}$ will be again smaller if a fixed premagnetization time T_{Premag} is assumed. This results in an increasingly asymmetric flux swing until the condition $\Delta E_{Pulse} = E_{Losses}$ is fulfilled, where the system stabilizes to the reset capacitor voltage $V_{CR,stable}$.

$$V_{CR,stable} = \frac{L_{mag}}{T_{Premag}} \left(\frac{\Delta I_{mag}}{2} - \frac{\Delta E_{Pulse}}{L_{mag} \Delta I_{mag}} \right) \tag{9}$$

In order to achieve a desired capacitor voltage $V_{CR,stable}$ the

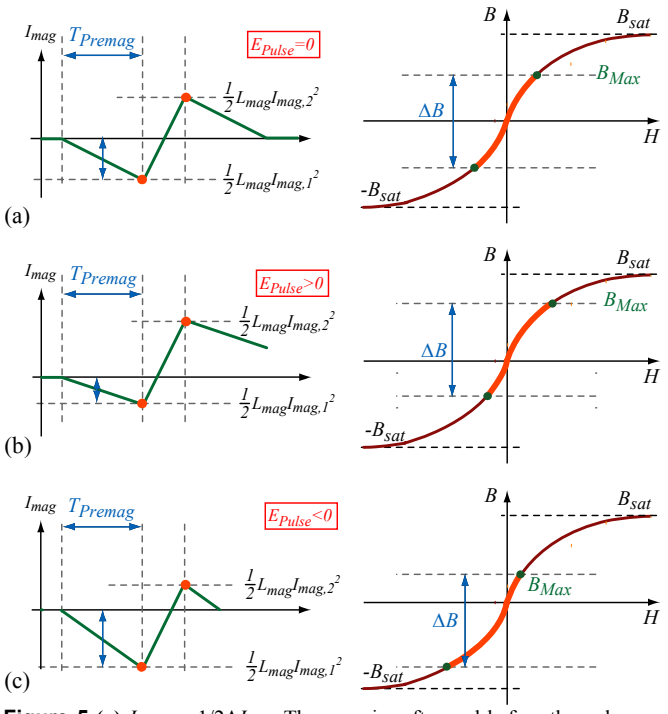

Figure 5 **(a)** $I_{Mag,1} = 1/2\Delta I_{Mag}$: The energies after and before the pulse are the same, **(b)** $I_{Mag,1} < 1/2\Delta I_{Mag}$: The energy after the pulse is the higher than the energy before the pulse and **(c)** $I_{Mag,1} > 1/2\Delta I_{Mag}$: The energy after the pulse is the lower than the energy before the pulse.

duration of T_{Premag} has to be adjusted depending on the resulting system losses E_{Losses}. Based on (9), longer premagnetization intervals T_{Premag} lead to a lower capacitor voltages $V_{CR,stable}$ and vice versa.

For relatively small system losses E_{Losses}, the active reset circuit can be operated with a fixed premagnetization interval T_{Premag}, which results in a slightly asymmetric flux swing and therefore in a slightly larger core cross section A_{Fe}. There, the system losses are compensated by the additional energy ΔE_{Pulse}, which is stored in the magnetizing inductance during the pulse. If the active reset circuit is self-stabilizing, the reset capacitor C_R has not to be precharged, because at start up due to the more asymmetric flux swing more energy will be recovered and therefore the reset capacitor will be charged to $V_{CR,stable}$ by the system itself. There, the pulse length/voltage must be limited in order to avoid core saturation.

3.1 PREMAGNETIZATION VOLTAGE STABILITY

To ensure stable operation of the system during self-regulation the power modulator with the active reset circuit specified in Table 2 has been analysed.

First, for each interval T_{Premag}, T_{Pulse} and T_{Demag} the system is simplified to a linear equivalent circuit, which corresponds to a damped LC-oscillator for the pre-/demagnetization interval T_{Premag} respectively T_{Demag} (cf. Figure 6). There, the copper and core losses of the system respectively of the transformer are considered with R_{Cu} and R_{Fe}.

Each pulse cycle starts with the premagnetization interval T_{Premag}, where the reset capacitor voltage V_{CR} has to be bigger or equal zero (cf. Figure 6 a)). Assuming $V_{CR} > 0$, during T_{Premag} the stored energy in the reset capacitor C_R will be transferred to the magnetizing inductance L_{Mag}. The according current and voltage waveforms during T_{Premag} for this LC-oscillation are shown in Figure 6 d). To guarantee proper operation of the active reset circuit, the capacitor voltage V_{CR} must stay positive until the end of T_{Premag}. Otherwise energy would be transferred back from the magnetizing inductance L_{Mag} to the reset capacitor C_R. Therefore, the duration of the premagnetization interval T_{Premag} is limited to $T_{Premag,max}$ (cf. Figure 6 d)). For the system specified in Table 1 and Table 2 the maximum duration $T_{Premag,max}$ of the premagnetization interval can be approximately calculated with (10).

$$T_{Premag,max} = \frac{\pi}{2}\sqrt{L_{Mag}C_R} = \frac{\pi}{2}\sqrt{2.5\mu H \cdot 240\mu F} = 38.4\mu s \quad (10)$$

To calculate the energy, which will be stored in the magnetizing inductance L_{Mag} during T_{Pulse} the system can be simplified by an ideal voltage source V_{pulse} and the magnetizing inductance L_{Mag} (cf. Figure 6 b)). Afterwards, during the demagnetization time T_{Demag} the stored energy in L_{Mag} will be transferred back to the reset capacitor C_R (cf. Figure 6 c)).

As presented in [11] the stability of a switched mode power supply system can be proven by deriving the linearized discrete small signal model of the system, where all poles of the resulting transfer function lie in the unit circle. Unfortunately, due to the large signal excitation in the considered power modulator with the active reset circuit this approach leads to inaccurate and unreliable results.

Therefore, the differential equations of the equivalent circuit for each individual interval T_{Premag}, T_{Pulse} and T_{Demag} are solved and the end values of the previous interval are consecutively used as initial values for the next interval to calculate the discrete waveform of the capacitor voltage V_{CR} during several pulses. In Figure 7 a) the step responses for two different initial capacitor voltages $V_{CR}(0) = 0V$ and $V_{CR}(0) = 400V$ are shown. As can be seen, the capacitor voltage V_{CR} is self-regulated after 7 pulses to the same voltage $V_{CR,stable} \approx 180V$ independent whether the initial capacitor voltage $V_{CR}(0)$

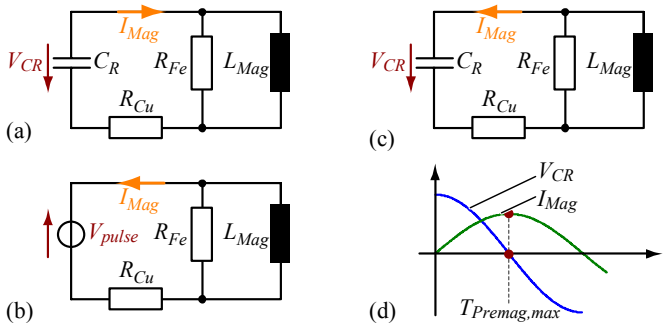

Figure 6 Simplified equivalent circuits during **(a)** the premagnetization interval T_{Premag}, **(b)** the pulse duration T_{Pulse} and the **(c)** demagnetization interval T_{Demag}. **(d)** magnetizing current I_{Mag} and reset capacitor voltage V_{CR} during the premagnetization interval T_{Premag}.

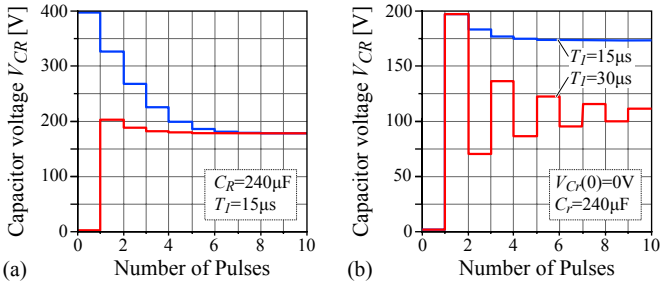

Figure 7 Self-regulation of the capacitor voltage V_{CR} during 10 Pulses for **(a)** the two initial capacitor voltages $V_{CR}(0) = 0V$ and $V_{CR}(0) = 400V$ and **(b)** for two different capacitance values $C_R = 240\mu F$ and $C_R = 480\mu F$.

is above or below the final value $V_{CR,stable}$.

Figure 7 b) shows the influence of the duration T_{Premag} on the step response of the capacitor voltage V_{CR}, where a longer duration of the premagnetization interval $T_{Premag} = 30\mu s$ leads to larger oscillations of the capacitor voltage V_{CR} compared to a shorter duration of $T_{Premag} = 15\mu s$. Due to the initial voltage of $V_{CR}(0) = 0V$ the core can not be premagnetized before the first pulse is generated. Therefore, the core is excited unidirectional during the first pulse and a lot of energy can be recovered in the reset capacitor C_R after the pulse.

In case of a long duration of T_{Premag} (T_{Premag} larger than $\approx 0.7T_{Premag,max}$) almost all of the recovered energy is again transferred back to the magnetizing inductance L_{Mag} before the second pulse and almost no energy is recovered after the second pulse. Due to the small energy stored in the capacitor C_R the core is premagnetized only a little before the third pulse is generated. Therefore, after the third pulse a lot of energy is recovered in the capacitor C_R again. Consequently, a long duration of the premagnetization interval T_{Premag} results in large energy oscillations between the reset capacitor C_R and the magnetizing inductance L_{Mag} until the voltage stabilizes to $V_{CR,stable}$. In order to achieve a step response without excessive oscillations, the duration T_{Premag} has to be reduced. Alternatively, the capacitance of the reset capacitor C_R could be increased or the system has to be ramped up from smaller pulse widths/voltages to the nominal pulse width/voltage.

3.2 NONLINEARITIES

So far, the nonlinearities, the saturation, the hysteresis and the remanence flux density of the core material have been neglected. In systems, where these effects are considered, the stability can not explicitly be proven. Therefore, the behavior

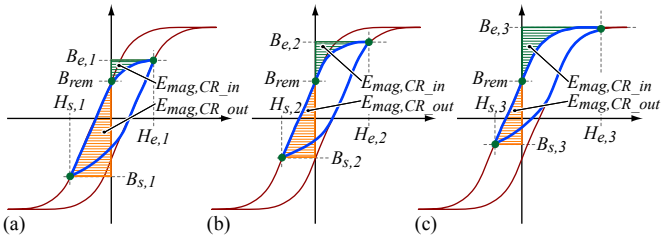

Figure 8 **(a)** Hysteresis-loop during the first pulse, where $E_{mag,CR\_out} >> E_{mag,CR\_in}$, **(b)** hysteresis-loop during the second pulse, where $E_{mag,CR\_out} > E_{mag,CR\_in}$ and **(c)** hysteresis-loop during the third pulse, where $E_{mag,CR\_out} \geq E_{mag,CR\_in}$.

of the system during self-regulation is analyzed with the hysteresis-loop of three consecutive pulse cycles. (cf. Figure 8).

Generally, the magnetic energy E_{mag} stored in an inductor can be expressed by the area between the hysteresis loop and the y-axis multiplied by the core volume, where l_{Fe} is the magnetic length and A_{Fe} is the cross section of the core.

$$E_{mag} = l_{Fe} A_{Fe} \int H(B) \mathrm{d}B \qquad (11)$$

There, the magnetic energy E_{mag} depends very much on the flux density B. In cases, where the flux swing ΔB is getting more asymmetric (i.e. when $|B_{s,i}| < |B_{e,i}|$, $i > 1$) additional energy is stored in the magnetizing inductance during the pulse and therefore more energy ($E_{mag} \approx B_e^2$) is transferred back to the reset capacitor C_R after the pulse compared to the energy ($E_{mag} \approx B_s^2$), which was transferred from the reset capacitor C_R to the magnetizing inductance before the pulse.

Due to the additional energy stored in the reset capacitor C_R, where $V_{CR} > V_{CR,nom}$, with a fixed duration of the premagnetization interval T_{Premag} the core will be more premagnetized (i. e. $|I_{Mag,1}| > |I_{Mag,2}|$) for the next pulse (cf. E_{mag,CR_out} in Figure 8 a)), which leads to a smaller flux density $B_{e,1}$ at the end of the first pulse and therefore to a smaller energy E_{mag,CR_in} recovered after the pulse.

Therefore, the core will be less premagnetized before the next pulse (cf. E_{mag,CR_out} in Figure 8 b)), but more energy E_{mag,CR_in} is recovered after the pulse. As soon as the energy E_{mag,CR_out} transferred to the magnetizing inductance L_{Mag} is equal to the energy E_{mag,CR_in} fed back to the reset capacitor C_R an equilibrium is reached, if the losses E_{Losses} of the system are neglected (cf. Figure 8 c)).

Otherwise, if additional losses E_{Losses} are considered the stored energy E_{mag,CR_in} in the magnetizing inductance L_{Mag}, which will be transferred to the reset capacitor C_R after the pulse, has to be larger than the energy E_{mag,CR_out}, which is used to premagnetize the core, to compensate the losses E_{Losses}. This leads then to a more asymmetric flux swing.

Finally, the asymmetry of the flux swing also depends on the remanence flux density B_{rem}. In order to achieve a large area between the hysteresis and the y-axis a small remanence

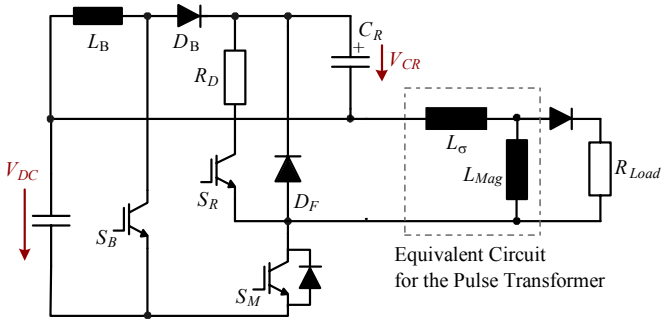

Figure 9 Schematic of the measurement setup for the active premagnetization and the DC/DC supply.

B_{rem} is needed to recover enough energy E_{mag,CR_in}. Contrariwise, for a large remanence $B_{rem} \approx B_{sat}$ the area between the hysteresis and the y-axis will be small and almost no energy E_{mag,CR_in} can be recovered.

4 FLUX SWING CONTROL OF THE ACTIVE RESET CIRCUIT

For larger losses E_{Losses} or high remanence flux densities B_{rem}, the active reset circuit can no longer be operated with self-regulation, because the more asymmetric flux swing can lead to saturation of the transformer core or a significantly larger core area is required. Therefore, the system losses E_{Losses} have to be compensated by a DC/DC power supply, which regulates the capacitor voltage V_{CR} to a fix value $V_{CR,nom}$. Additionally, a control loop has to be implemented, which results in a symmetric flux swing in the transformer core.

In Figure 9 the schematics of the power modulator system with the added DC/DC power supply is shown. There, a DC/DC boost converter, transferring energy from the input capacitor C_{in} to the reset capacitor C_R, is added to the system to recharge the reset capacitor C_R to the nominal capacitor voltage $V_{CR,nom}$. For changing the magnetization level $I_{Mag,1}$ for a constant capacitor voltage $V_{CR,nom}$ the duration of the premagnetization interval T_{Premag} has to be adjusted (cf. (2)).

In the same manner, the demagnetization interval T_{Demag} is defined by the magnetization current $I_{Mag,2}$ at the end of the pulse and the resulting back EMF, which is approximately equal to the reset capacitor voltage V_{CR} plus the forward voltage of the freewheeling diode V_{DF}.

$$T_{Demag} = \frac{L_{Mag} \cdot I_{Mag,2}}{V_{CR} + V_{DF}} \tag{12}$$

If the core is excited symmetrically from $-I_{Mag}$ to I_{Mag}, i.e. $|I_{Mag,1}| = |I_{Mag,2}|$, if the capacitor voltage V_{CR} is regulated and if the forward voltage V_{DF} is neglected compared to V_{CR}, the durations of T_{Premag} and T_{Demag} are equal (cf. Figure 10). Consequently, for asymmetric excitation the duration of T_{Demag} will be shorter than T_{Premag} if $|I_{Mag,1}| > |I_{Mag,2}|$ and contrariwise, the duration T_{Demag} will be longer than T_{Premag} for $|I_{Mag,1}| < |I_{Mag,2}|$ as shown in Figure 10 b) and Figure 10 c).

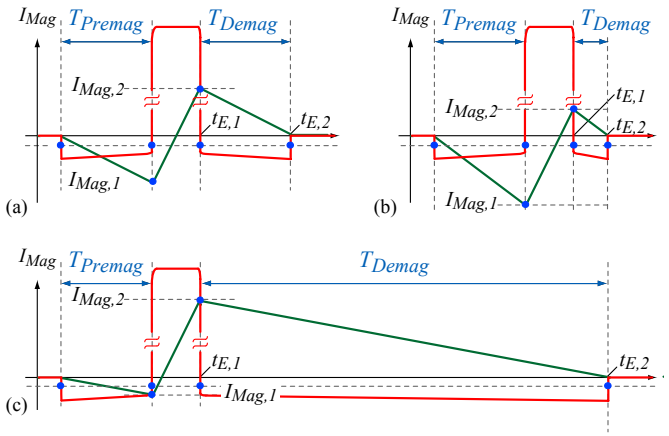

Figure 10 **(a)** Symmetric flux swing, where $T_{Premag} = T_{Demag}$, **(b)** and **(c)** asymmetric flux swing, where $T_{Premag} > T_{Demag}$ respectively $T_{Premag} < T_{Demag}$.

Table 2 Components of the active reset circuit for one of four pulse generator units.

S_R	SMK400GAL176D	1700V / 430A	Semikron
D_F	DH60-18A	1800V / 60A	IXYS
C_R	B32524Q3106	10µF / 250V	Epcos

Therefore, to achieve a symmetric flux swing in the transformer core the premagnetization time T_{Premag} has to be controlled in such a way that $T_{Premag} = T_{Demag}$ is achieved (cf. Figure 10). There, the duration of T_{Demag} can be measured by detecting the edge times $t_{E,1}$ and $t_{E,2}$ of the negative primary voltage with an high speed comparator (cf. Figure 10).

5 DESIGN AND EXPERIMENTAL RESULTS

In Figure 11 a) a picture of the pulse generator prototype containing the main switch S_M and the active reset circuit is shown. There, the input capacitors C_{in} and the bus bar connections to the pulse transformer would be mounted on the top as shown in Figure 1. The whole power modulator consists of four equal pulse generator units (cf. Figure 1 and Figure 11 a)), where each is connected to one primary of the pulse transformer. Due to the maximum allowed negative klystron voltage of -50kV the reset capacitor voltage V_{CR} was set to 150V in the considered case, which results in a secondary voltage of -30kV.

The switch S_R of the active reset circuit for one pulse generator was realized with a single IGBT Module, which has to carry a peak current of 250A (= 1000A/4 pulse generator units). For the freewheeling diode D_F six parallel discrete diodes were used to achieve a low inductive freewheeling path. The reset capacitor C_R was built with six parallel foil capacitors, which also guarantee a low inductive design and a high current capability. The selected components for the active reset circuit of one pulse generator unit are listed in Table 2.

In the test circuit a series connection of a resistor and a

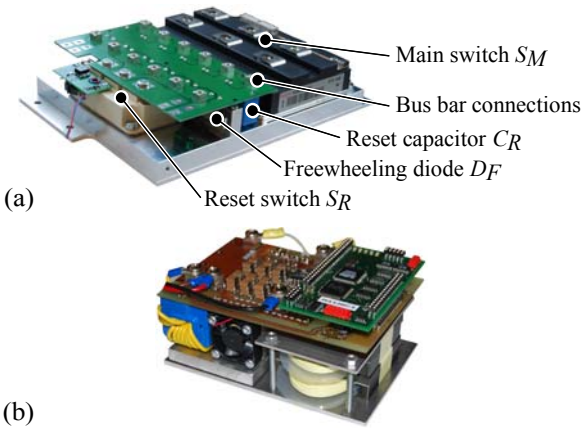

Figure 11 **(a)** Prototype of the active reset circuit and **(b)** DC/DC boost converter (V_{in}=1000V, V_{out} = 0…200V, P_{out}=1kW).

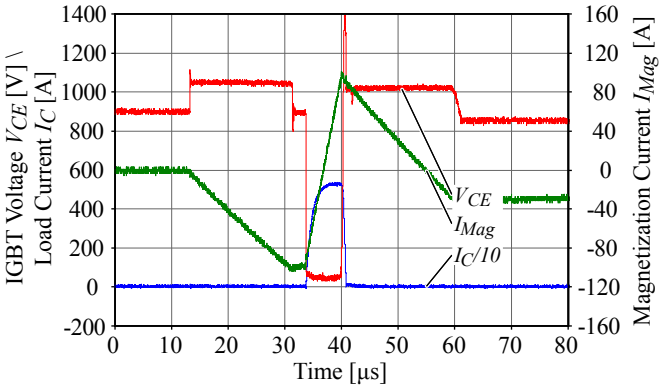

Figure 12 Symmetric flux swing, where $T_{Premag} \approx T_{Demag}$.

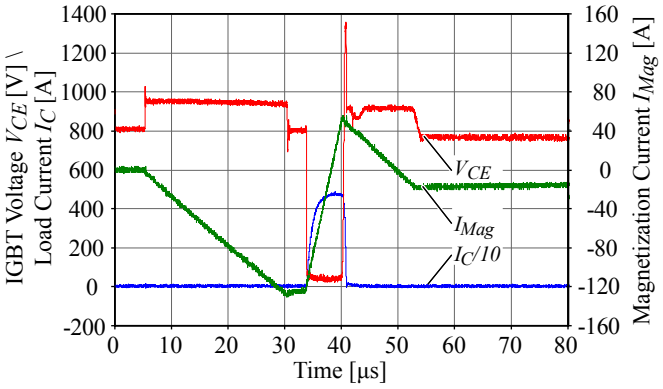

Figure 13 Asymmetric flux swing, where $T_{Premag} > T_{Demag}$.

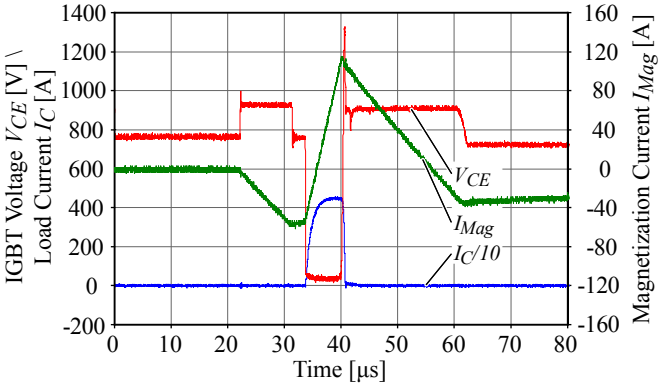

Figure 14 Asymmetric flux swing, where $T_{Premag} < T_{Demag}$.

diode was used instead of a klystron. For a magnetizing current of I_{Mag}=1000A the resulting klystron voltage V_k' reflected to the primary is approximately 60V, which leads to a slow decay of the premagnetizing current I_{Mag} during the interlocking delay. Therefore, the interlocking delay was selected to be 3µs to avoid an intersection of the turn off of S_R and the turn on of S_M.

In order to test the flux control of the active reset circuit the transformer with the magnetizing inductance was replaced by an inductor equivalent to the magnetizing inductance L_{Mag}. For the measurements the inductor was realized with two tape wound C-cores (size: CC25, tape: 50µm) of a 3% SiFe alloy, due to the high saturation flux density B_{sat}. Additional measurements also have done with the amorphous 2605SA1 (size: AMCC25, tape: 25µm).

In Figures 12, 13 and 14 the measured magnetizing current I_{Mag}, the IGBT current I_C and the IGBT voltage V_{CE} for a symmetric and two asymmetric flux swings are shown. For the symmetric flux/current swing it can be seen, that the durations of the two magnetization times T_{Premag} and T_{Demag} are almost equal. The relative error results due to the forward voltage drop and the reverse recovery time of the used freewheeling diode D_F. As expected, the demagnetization time T_{Demag} will become shorter if $I_{Mag,1}$ is getting larger (cf. Figure 13). Contrariwise the demagnetization time T_{Demag} will be longer if $I_{Mag,1} < I_{Mag,nom}$ (cf. Figure 14). Additionally, the waveform of V_{CE} shows a very short negative peak when S_M is turned off, which is caused by the current flowing through the leakage inductance L_σ and the input stage.

In Figure 15 and Figure 16 the measured magnetizing current I_{Mag} and the induced voltage V_{ind} for self-regulation and symmetric flux swing are shown. Additionally, with the measured values I_{Mag} and V_{ind} the according hysteresis-loop was calculated (cf. Figure 15 b) and Figure 16 b)). As explained in section 3, the active reset with self-regulation results in an asymmetric flux swing, where the energy E_{mag,CR_in} stored in the magnetizing inductance after the pulse has to be larger than the energy E_{mag,CR_out}, which is used to premagnetize the core, because the losses E_{Losses} of the system has to be compensated. In order to achieve a symmetric flux swing the flux control as described in section 4 has to be applied. In Figure 16 b) the resulting hysteresis-loop for the active reset circuit with flux control is shown. There, the energies E_{mag,CR_in} and E_{mag,CR_out} are almost equal. However, to achieve a symmetric flux swing ($-B_s = B_e$) an equality of E_{mag,CR_in} and E_{mag,CR_out} is not necessary and depends on the core material as well as on the pulse shape.

6 CONCLUSION

In this paper a detailed description of the active reset circuit operation principle and the control is given. It is shown that for systems, with low losses, the active reset circuit balances the flux swing in the transformer core automatically. In this case the premagnetization time T_{Premag} can be set to a fix value.

In systems with higher losses an additional boost converter, which compensates the losses related to the premagnetization and which stabilizes the reset capacitor voltage V_{CR}, is required in order to achieve a symmetric flux swing. Additionally a new and simple control method of the premagnetization interval T_{Premag} is presented, which provides symmetric flux swings.

For validating the presented results a prototype with a pulsed power of 20MW, a pulse voltage of 200kV and a maximum pulse width of 5µs has been built. The obtained measurement results correspond very well with the theoretical predictions and show that the losses in the premagnetization could be drastically reduced by about 80% with an active reset circuit compared to a passive reset circuit.

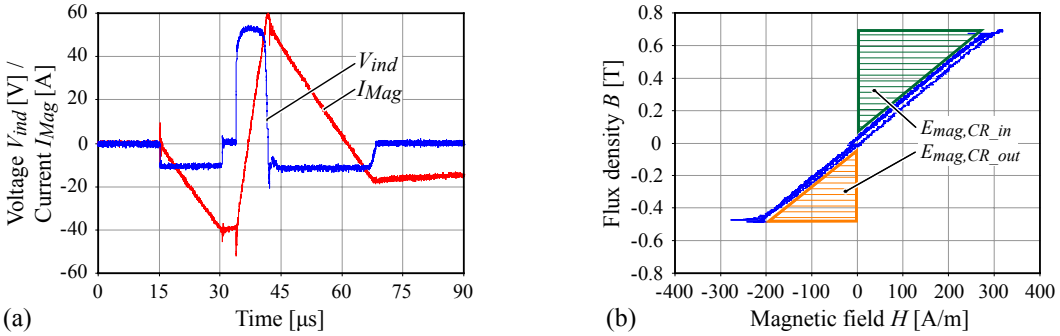

Figure 15 **(a)** Asymmetric flux swing, where $T_{Premag} > T_{Demag}$ and **(b)** the associated hysteresis loop, where $E_{mag,CR\_in} > E_{mag,CR\_out}$.

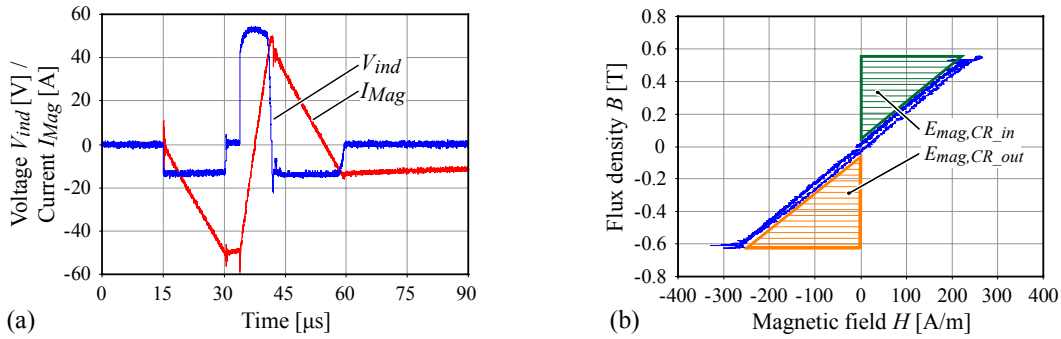

Figure 16 **(a)** Symmetric flux swing, where $T_{Premag} \approx T_{Demag}$ and **(b)** the associated hysteresis loop, where $E_{mag,CR\_in} \approx E_{mag,CR\_out}$.

REFERENCES

[1] E. G. Cook, F. V. Allen, E. M. Anaya, E. J. Gower, S. A. Hawkins, B. C. Hickman, B. S. Lee, J. S. Sullivan, J. A. Watson, C. A. Brooksby, J. Yuhas, R. Cassel, M. Nguyen, C. Pappas and J. De Lamare, "Solid-State Modulator R&D at LLNL," International Workshop on Recent Progress of Induction Accelerators, Tsukuba, Dez. 2002

[2] S. Ashby, D. Drury, G. James, P. Sincerny, L. Thompson and L. Schlitt, "CLIA - A compact Linear Induction Accelerator System," Records of IEEE 8th Pulsed Power Conference, pp. 940-942, June 1991

[3] D. Bortis, J.Biela, J.W. Kolar, "Optimal Design of a DC Reset Circuit for Pulse Transformers," Records of IEEE 22nd Applied Power Electronics Conference, APEC 2007, pp. 1171-1177, Anaheim, CA, Feb. 2007

[4] H. Kirbie, "Unified Power Architecture," U.S. Patent No.: 6,529,387, March 4, 2003.

[5] Kirbie, "Unified Power Architecture with Dynamic Reset," U.S. Patent No.: 6,466,455, October 15, 2002.

[6] P. Vinciarelli, "Optimal Resetting Of the Transformer's Core in single ended Forward Converters," Patent US4441146, Vicor Corporation, 3, April 1984, Westford, Mass.

[7] Q. Li, F. C. Lee, M. M. Jovanovic, "Design Consideration of Transformer DC Bias of Forward Converter with Active-Clamp Reset," Proceedings of IEEE 15th Applied Power Electronics Conference, APEC 00, Page(s): 966-972, 2000, New Orleans (USA).

[8] J. Biela, D. Bortis, J.W. Kolar, "Reset Circuits with Energy Recovery for Solid State Modulators," Proceedings of IEEE 16th Pulsed Power and Plasma Science Conference, PPPS 2007, pp. 1309-1312, Albuquerque, NM, June 2007

[9] J. S. Oh, W. Namkung, K.H. Chung, T. Shintake and H. Matsumoto, "Rise time analysis of pulsed klystron-modulator for efficiency improvement of linear colliders," Nuclear Instruments and Methods in Physics Research Section A, Volume 443, Issue 2-3, p. 223-230, April 2000.

[10] G. Caryotakis, "High Power Klystrons: Theory and Practice at the Stanford Linear Accelerator Center," SLAC-PUB, 2004.

[11] I. Batarseh, K. Siri, "Generalized Approach to the Small Signal Modeling of DC-to-DC Resonant Converters," IEEE Transaction on Aerospace and Electronic Systems, Volume 29, Issue 3, p. 894-909, July 1993.

Dominik Bortis (S'06) was born in Fiesch, Switzerland on December 29, 1980 He studied electrical engineering at the Swiss Federal Institute of Technology (ETH) Zurich. During his studies he majored in communication technology and automatic control engineering. In his diploma thesis he worked with the company Levitronix, where he designed and realized a galvanic isolation system for analog signals. He received his M.Sc. degree in May 2005, and he has been a Ph.D. student at the Power Electronic Systems Laboratory, ETH Zürich, since June 2005.

Juergen Biela (S'04) studied electrical engineering at the FAU Erlangen, Germany. During his studies he dealt in particular with resonant DC-link inverters at the Strathclyde University, Scotland and the active control of series connected IGCTs at the Technical University of Munich. After he had received his diploma degree with honors from FAU Erlangen in October 2000, he worked on inverters with very high switching frequencies, SiC components and EMC at the research department of A&D Siemens, Germany. From July 2002 he has been a Ph.D. student at the PES, ETH Zurich and since January 2006 he is PostDoc.

Johann W. Kolar (M'89 SM'02) studied industrial electronics at the University of Technology Vienna, Austria, where he also received the Ph.D. degree (summa cum laude). From 1984 to 2001 he was with the University of Technology in Vienna, where he was teaching and working in research in close collaboration with industry. He has proposed numerous novel converter topologies, e.g., the VIENNA Rectifier and the Three-Phase AC-AC Sparse Matrix Converter concept. Dr. Kolar has published over 200 scientific papers in international journals and conference proceedings and has filed more than 50 patents. He was appointed Professor and Head of the Power Electronics Systems Laboratory at the ETH Zurich on Feb. 1, 2001.